Ionospheric electron heating, optical emissions, and striations induced by powerful HF radio waves at high latitudes: Aspect angle dependence

M. T. Rietveld,[1,6] M. J. Kosch,[2,7] N. F. Blagoveshchenskaya,[3] V. A. Kornienko,[3] T. B. Leyser,[4] and T. K. Yeoman[5]

Received 18 June 2002; revised 26 November 2002; accepted 9 January 2003; published 3 April 2003.

[1] In recent years, large electron temperature increases of 300% (3000 K above background) caused by powerful HF-radio wave injection have been observed during nighttime using the EISCAT incoherent scatter radar near Tromsø in northern Norway. In a case study we examine the spatial structure of the modified region. The electron heating is accompanied by ion heating of about 100 degrees and magnetic field-aligned measurements show ion outflows increasing with height up to 300 m s^{-1} at 582 km. The electron density decreases by up to 20%. When the radar antenna was scanned between three elevations from near field-aligned to vertical, the strongest heating effects were always obtained in the field-aligned position. When the HF-pump beam was scanned between the same three positions, the heating was still almost always strongest in the field-aligned direction. Simultaneous images of the 630 nm O(^{1}D) line in the radio-induced aurora showed that the enhancement caused by the HF radio waves also remained localized near the field-aligned position. Coherent HF radar backscatter also appeared strongest when the pump beam was pointed field-aligned. These results are similar to some Langmuir turbulence phenomena which also show a strong preference for excitation by HF rays launched in the field-aligned direction. The correlation of the position of largest temperature enhancement with the position of the radio-induced aurora suggests that a common mechanism, upper-hybrid wave turbulence, is responsible for both effects. Why the strongest heating effects occur for HF rays directed along the magnetic field is still unclear, but self-focusing on field-aligned striations is a candidate mechanism, and possibly ionospheric tilts may be important. *INDEX TERMS:* 2403 Ionosphere: Active experiments; 6929 Radio Science: Ionospheric physics (2409); 7839 Space Plasma Physics: Nonlinear phenomena; *KEYWORDS:* HF-heating, ionospheric modification, electron heating, EISCAT, striations, aspect angle

Citation: Rietveld, M. T., M. J. Kosch, N. F. Blagoveshchenskaya, V. A. Kornienko, T. B. Leyser, and T. K. Yeoman, Ionospheric electron heating, optical emissions, and striations induced by powerful HF radio waves at high latitudes: Aspect angle dependence, *J. Geophys. Res.*, *108*(A4), 1141, doi:10.1029/2002JA009543, 2003.

1. Introduction

[2] Electron temperature enhancements caused by powerful HF wave injection experiments have been measured by incoherent scatter radars many times since the first observations by *Gordon et al.* [1971] and *Gordon and Carlson* [1974]. Nighttime observations of electron heating at Arecibo [*Mantas et al.*, 1981] showed enhancements of some 40% (about 350 K) which could be explained by a comprehensive numerical model. It was found that about half the heating was caused by anomalous absorption and half by deviative absorption. Experiments done at night in winter at solar minimum using an HF frequency of 3.175 MHz showed much larger enhancements of about 1000 to 2000 K [*Djuth et al.*, 1987, *Duncan et al.*, 1988] which were explained by the much lower cooling rates caused by poor thermal coupling between the lower density plasma and the neutral atmosphere [*Newman et al.*, 1988]. The only other facility where HF-induced electron heating has been directly measured using incoherent scatter is EISCAT, in the high-latitude region. Most measurements were made during the daytime [*Jones et al.*, 1986; *Stocker et al.*, 1992; *Honary et al.*, 1993, 1995; *Robinson et al.*, 1996] when the ionosphere is most stable and similar to that at midlatitudes. Temperature increases up to about 55% (about 700 K) and electron density increases of up to

[1]Max-Planck Institut für Aeronomie, Katlenburg-Lindau, Germany.
[2]Communication Systems, Lancaster University, Lancaster, UK.
[3]Arctic and Antarctic Research Institute, St. Petersburg, Russia.
[4]Swedish Institute of Space Physics, Uppsala, Sweden.
[5]Physics and Astronomy, Leicester University, Leicester, UK.
[6]Also at EISCAT, Ramfjordmoen, Ramfjordbotn, Norway.
[7]Also Honorary Research Fellow, University of Natal, Durban, South Africa.

0148-0227/03/2002JA009543$09.00

about 15% near the HF wave interaction height of 185 km were measured. They examined several different days where the HF beam was vertical and other days when the beam was near field-aligned, but no comparison between the results for different HF beam directions was made. *Honary et al.* [1993] examined temporal fluctuations in the electron temperature and electron density and concluded that they were driven by chemical perturbations rather than the self-focusing instability found in transport dominated regions at higher altitudes.

[3] There is a close association between HF-induced electron heating, the generation of artificial small-scale field-aligned irregularities (AFAI) [*Fialer*, 1974; *Minkoff et al.*, 1974] and the phenomenon known as anomalous absorption [*Robinson*, 1989; *Robinson et al.*, 1996]. An O-mode HF wave couples through either pre-existing or artificially induced field-aligned electron density striations into electrostatic (upper hybrid) waves at the upper-hybrid resonance (UHR) height. These waves propagate near perpendicular to the magnetic field and dissipate energy thereby heating the electron gas. The upper hybrid waves can, due to thermal nonlinearities, excite filamentary density perturbations or striations which can trap the exciting upper hybrid field. Early theories concerned the initial thermal parametric instability [*Grach and Trakhtengerts*, 1976] and the resonance instability [*Vas'kov and Gurevich*, 1976]. More recently the nonlinear stabilization of the striations was studied [*Gurevich et al.*, 1995], including both the thermal parametric and the resonance instability [*Istomin and Leyser*, 1997]. These models are consistent with in situ rocket measurements at mid latitudes of the depletion depth (6%) and width (7 m) of small-scale striations [*Kelley et al.*, 1995; *Franz et al.*, 1999]. The result is efficient transfer of energy from the HF wave into heat and the accompanying absorption of diagnostic HF waves is known as anomalous absorption [*Gurevich et al.*, 1996].

[4] The rocket data showed that the striations exist in bunches of about 1–2 km with similarly sized regions of no striations in between. This bunching of striations has been interpreted in terms of nonlinear self-focusing of the HF wave including the effect of trapping of the HF wave in large-scale density irregularities [*Gurevich et al.*, 1999]. The bunching of striations can also occur simply by diffraction of the HF wave on the small-scale striations [*Istomin and Leyser*, 2001]. Further, experimental results on HF-induced optical emissions at high latitudes with its southward displacement of the glow cloud [*Brändström et al.*, 1999; *Kosch et al.*, 2000; *Pedersen and Carlson*, 2001] and the associated large electron temperature enhancements [*Leyser et al.*, 2000; *Gustavsson et al.*, 2001] has also been interpreted in terms of the nonlinear self-focusing of the HF wave in which the bunches of small scale striations are soliton-like nonlinear structures [*Gurevich et al.*, 2001].

[5] It has been found that the temperature enhancements, like anomalous absorption and other phenomena related to UH waves, also exhibit a dependence on the difference between pump frequency and gyrofrequency harmonic [*Honary et al.*, 1995; *Robinson et al.*, 1996]. In particular, the heating was closely related to anomalous absorption and both showed a strong minimum when the pump frequency was near the third and fourth harmonic of the electron gyrofrequency. This last result in particular is very significant because it directly relates the electron heating mechanism, like several other phenomena, to electrostatic instabilities. The anomalous absorption results near the third gyroharmonic could be explained by the nonlinear theory of *Gurevich et al.* [1996]. In addition, the intensity of small-scale striations has a minimum at the gyroharmonics [*Honary et al.*, 1999; *Ponomarenko et al.*, 1999]. More recently it was discovered that radio-induced red (630 nm) aurora also shows a minimum when pumping near a gyroharmonic [*Bernhardt et al.*, 2000; *Kosch et al.*, 2002a] as was predicted by *Gurevich and Milikh* [1997]. This clearly links radio-induced heating and optical emission to the same mechanism involving upper-hybrid waves and striations.

[6] Until recently, very few EISCAT measurements of HF-modification effects in the F region were made at night. The reason for this is that at night in the auroral region the F region plasma density is often too low (under-dense) for the HF wave to interact effectively with the plasma. Furthermore, under disturbed auroral conditions, particle precipitation may cause the E- and D-region plasma densities to be too high, either reflecting or absorbing the HF wave. Under solar maximum and quiet magnetic conditions, however, these obstacles are less common, as the data here show.

[7] Since about October 1998, near the start of a maximum in the sunspot cycle, it was noticed that electron densities were often high enough ($>2 \times 10^{11}$ m^{-3} such that the plasma frequency exceeded the lowest useable HF frequency of 4 MHz) in the F region at night such that HF-interaction experiments were possible, under relatively quiet geomagnetic conditions. A concerted effort was made to perform experiments at night with the result that from February 1999 radio-induced aurora, also referred to as artificial airglow, was produced and imaged at Tromsø [*Brändström et al.*, 1999]. The light emissions were associated with large (factor up to 3.5) electron temperature enhancements measured using the EISCAT UHF radar pointed along the magnetic field aligned direction [*Leyser et al.*, 2000; *Gustavsson et al.*, 2001]. Other radio-induced aurora results measured from Skibotn, 50 km to the east of the HF facility, showed a pronounced southward displacement of the glowing patch [*Kosch et al.*, 2000, 2002b, 2003]. Also radio-induced optical emissions measured at another high-latitude heating facility, HAARP, have shown a southward displacement [*Pedersen and Carlson*, 2001].

[8] This southward displacement of the emissions shows some similarity to other HF-interaction experiments [*Isham et al.*, 1999a, 1999b; *Mishin et al.*, 2001] where the aspect angle dependence of various Langmuir turbulence effects was measured. The experiments of Isham et al. used low duty cycle HF pulses to investigate the spatial occurrence of Langmuir and ion-acoustic waves measured by the EISCAT UHF (931 MHz) and to a lesser extent, VHF (224 MHz) incoherent scatter radars. When the center of the relatively wide HF beam was pointed 6° south, it was found that several phenomena were most pronounced when the narrow UHF radar beam was pointed between about 6° and 12° south of zenith, corresponding to angles between the Spitze and the field-aligned position.

[9] In view of all the above results which suggest that the F region approximately 50 km south of the HF facility is a preferred position for AFAI, radio-induced aurora, and some signatures of Langmuir turbulence, we decided to perform

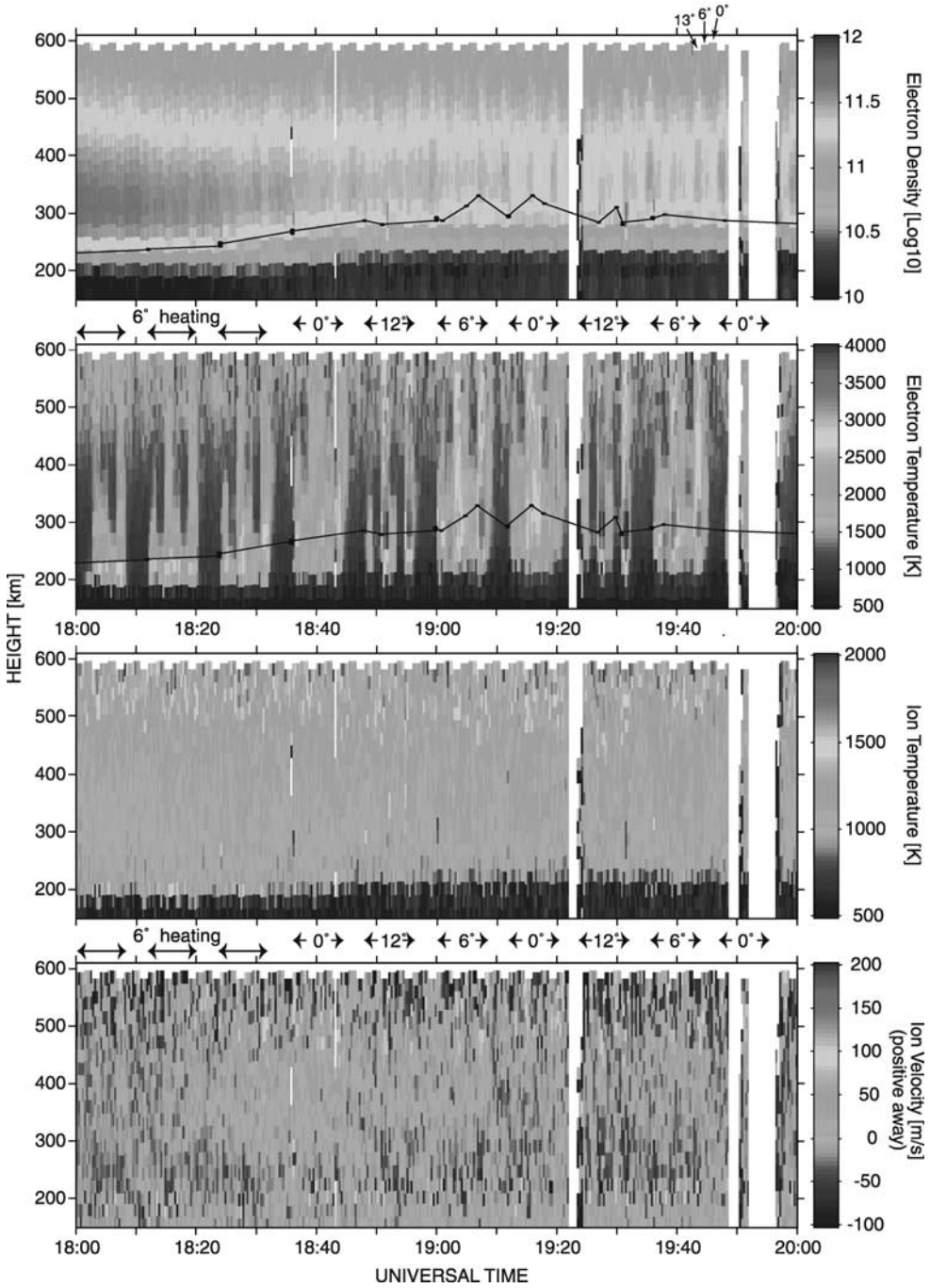

Figure 1. Data from the EISCAT UHF radar at Tromsø on 7 October 1999, obtained using the long-pulse and analyzed with 20 s integration time, showing the effects of HF pumping. The HF was cycled 8 min on, 4 min off, with the beam directed at southward zenith angles shown below the upper and above the lowest panels. The UHF antenna was continually scanned in a 4-min cycle between almost the same positions, 6°, 0°, 12.8° zenith angles, which are distinguishable by the varying upper altitude as labeled at the upper right of the first panel. The solid line in the upper two panels connects points indicating the HF-enhanced ion line (HFIL) height obtained from the two power profiles. The HFIL height should be close to but below the HF reflection height.

further experiments to see if the HF-induced electron temperature also shows a similar spatial dependence. This question arose because one of the postulated mechanisms for the enhanced light emission is that the excitation of the oxygen atoms is due to the Maxwellian tail of the heated electron distribution [e.g., *Mantas*, 1994; *Mantas and Carlson*, 1996], modified by the excitation of vibrational states in N_2 [*Mishin et al.*, 2000]. To this end, the UHF radar antenna would scan several positions covering most of the HF beam while measuring electron temperatures, and the HF beam

was also scanned through the same positions with a much slower cycle. The results of this experiment are presented below. At the same time observations of radio-induced aurora were made as well as striations by using coherent backscatter experiments with a unique bistatic HF Doppler scatter technique [*Blagoveshchenskaya et al.*, 1998] and the CUTLASS coherent backscatter radar [*Milan et al.*, 1997].

[10] We present data from an experiment on 7 October 1999 where both the HF-pump beam and the diagnostic radar beams were scanned in elevation between magnetic field-aligned and vertical directions. Some of the characteristics of the topside electron temperature effects such as propagation and ion temperature increases and outflow are discussed. Electron temperature data from the remote site stations of Kiruna and Sodankylä are used to show that for a given plasma volume there is no dependence of the measured electron temperature on direction of the radar beam to the magnetic field. Finally, we discuss the interpretation of the strong dependence of the heating on the HF incidence angle.

2. Experimental Details

2.1. HF Facility

[11] The EISCAT HF facility (69.59°N, 19.23°E) near Tromsø, in northern Norway [*Rietveld et al.*, 1993] was used to create large electron temperatures in the high-latitude F region during quiet geomagnetic conditions in the hours after sunset on 7 October 1999. The HF facility was operated at 4.544 MHz, O-mode with a modulation cycle of 8 min on followed by 4 min off. All 12 transmitters were used at 80 kW each, using array 2 resulting in a gain of 23.3 dBi and an effective radiated power (ERP) of 205 MW. The width of the beam was 12° at the −3 dB point and was 16.6° at the −6 dB point. The HF modulation started at 1812 UT for a fixed direction of the HF beam at 6° south, but from 1824 until 2000 UT the HF beam zenith angle was scanned electronically with the following 36 min cycle: 8 min 6° (Spitze), 4 min off, 8 min 0° (vertical), 4 min off, 8 min 12° (field-aligned), 4 min off. Note that the HF frequency was well away from any gyrofrequency harmonic where a minimum in electron temperature enhancement has been found [*Robinson et al.*, 1996].

2.2. Radar Modulation

[12] The EISCAT UHF radar was used with CP-1-K modulation which involves a basic time resolution of 5 s and best altitude resolution of 3.1 km in power profile and alternating code data. A long pulse modulation also gives 21 range gates in the F region from 145 to 596 km with 22.5 km spacing and provides signal for tri-static observations at 250 km using the Kiruna and Sodankylä receiving stations.

3. Observations

3.1. Tromsø Observations of 7 October 1999

[13] Magnetic conditions were quiet. Ionograms from the Tromsø dynasonde showed that foF2 from 1910 to 1950 UT was of the order of 4.9 MHz. The tristatic ion velocity measurements from the EISCAT UHF radar showed westward ion drifts up to 200 m s^{-1} before about 1840 UT changing to eastward drifts of up to about 300 m s^{-1} afterwards. The north-south velocities are less than 100 m s^{-1} before 1840 UT after which they vary up to 200 m s^{-1}. Vector velocities derived from the HF sounder Doppler shifts show the magnetic east-west F region irregularity drifts to be westwards and less than 100 m s^{-1} between 1800 and 1845 UT, turning to eastwards and varying between 0 and 100 m s^{-1} up to 2000 UT. The north-south component has an average near zero with excursions between ±60 m s^{-1}. Why the HF sounder derived velocities appear to be smaller than the EISCAT velocities requires a more detailed analysis which is beyond the scope of this paper.

[14] Figure 1 shows the EISCAT data from Tromsø for between 1800 and 2000 UT on 7 October 1999 as the UHF radar beam was tilted from 0° zenith angle to 12.8° south to 6° south and back to 0° in a 4-min cycle, spending a maximum of 80 s per position. Figure 2 shows in more detail the same data as in Figure 1 for three positions of the HF beam from 1846 to 1922 UT. At the top of each panel are shown the UHF antenna zenith angles. Data taken during antenna movements are included in the 20 s integrated data in both figures.

[15] There are several features to note in the figures. Increases in electron temperature (second panel) are obvious throughout the 2-hour interval, and they get larger with time as the altitude of the F layer increases after sunset. There is a clear increase in the height of the F layer around 1825 UT. The HF-enhanced ion line (HFIL), which is excited at or close to but below the HF reflection height [e.g., *Rietveld et al.*, 2000], and which was often observed immediately after HF turn-on, is shown in the top panel by the solid line joining the measured points on the bottomside F layer. These measurements were made with the two power profiles giving a resolution of up to 3.1 km in range. The upper hybrid resonance (UHR) height, which is where the strongest heating is thought to take place, was estimated from the power profile data to be between 3 and 9 km below the reflection height.

[16] A striking feature is that for all three pointing directions of the UHF antenna, the electron temperature increases are larger when the HF beam is directed to 12° zenith angle (field-aligned) and become successively weaker for the 6° and 0° positions. Furthermore, the temperature increase is nearly always strongest at any given height when the UHF antenna is pointed at 12.8°, for all three positions of the HF beam.

[17] Although there are no obvious changes in electron density associated with the heating in the color plots, there are density depletions up to about 20% (about 4×10^{-10} m^{-3}) above about 200 km. The change in density with antenna position, evident in Figures 1 and 2, is caused by horizontal gradients in electron density. After about 1850 UT the density increases towards the south.

Figure 2. (opposite) A subset of the EISCAT UHF data from the 7 October 1999 data in Figure 1, showing more detail. The numbers near the top of each panel show the UHF antenna zenith angles, whereas those between the upper two and lower two panels show the HF beam zenith angles. The height of the HFIL is shown by the dots joined by solid lines in the upper two panels.

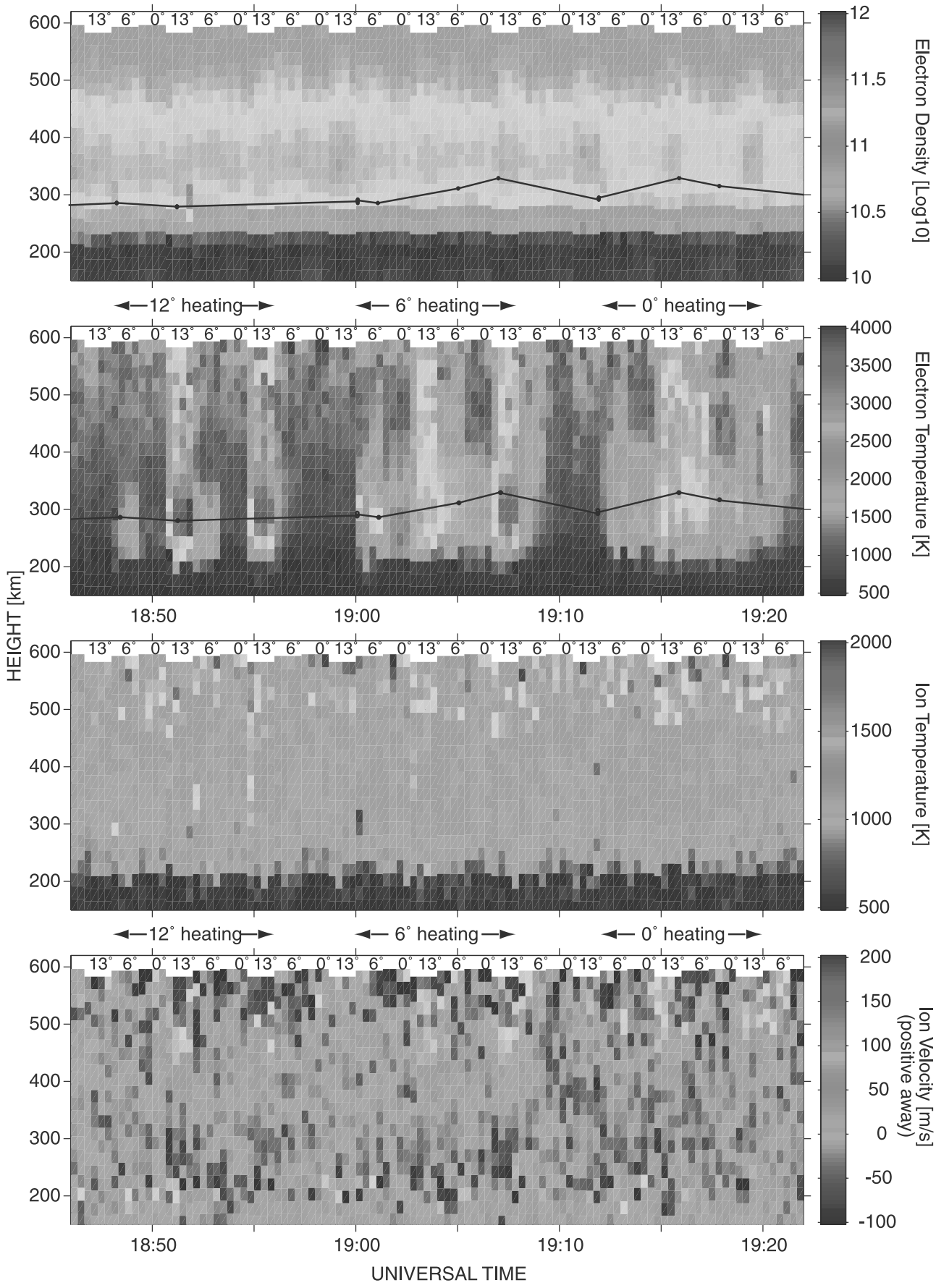
13° 6° 0° 13° 6° 0° 13° 6° 0° 13° 6° 0° 13° 6° 0° 13° 6° 0° 13° 6° 0° 13° 6° 0° 13° 6°
600
500
400
300
200
12
11.5
11
10.5
10
Electron Density [Log10]
◄—12° heating—►
◄— 6° heating —►
◄— 0° heating —►
4000
3500
3000
2500
2000
1500
1000
500
Electron Temperature [K]
HEIGHT [km]
18:50
19:00
19:10
19:20
2000
1500
1000
500
Ion Temperature [K]
200
150
100
50
0
-50
-100
Ion Velocity [m/s]
(positive away)
UNIVERSAL TIME

[18] The ion temperature increase (third panel) is modest, reaching about 100 degrees. Finally, there are ion outflows (bottom panel) reaching about 200–300 ms^{-1} above 400 km in the field-aligned position associated with the electron temperature increases.

[19] Figure 3 shows an example from the field-aligned position of profiles of the four main ionospheric parameters for the HF turned on in the field-aligned position, compared with when it was off. The clearest effects are seen in the electron temperature and in the ion velocity. Such ion outflows are often observed naturally in the auroral ionosphere, but have never been reported as a result of HF-pumping experiments. Ion outflows have long been predicted to be a result of HF-heating experiments as in papers by *Meltz and Lelevier* [1970], *Vas'kov et al.* [1993], and *Mingaleva and Mingalev* [1997].

3.2. Electron Temperature Enhancements

[20] From the three-position data in Figures 1 and 2, one can draw contour plots in the meridian plane of the electron temperature enhancements. Figure 4 shows typical contour plots of the electron heating for the three HF beam positions. In each plot the temperature data from three radar profiles in a 4-min interval associated with a given HF beam angle are combined into one contour plot. Although the contours are the result of interpolation between only three positions, the strong field-aligned nature of the heating is apparent. Extrapolation of the contours beyond the field-aligned position is not valid for the present 3-position data. Subsequent measurements in February 2001, which will be published separately, show that the temperature enhancement decreases for radar antenna positions beyond field-aligned.

[21] To show more quantitatively the dependence of electron temperature enhancement on the angle of the HF beam to the magnetic field, we plot in Figure 5 the maximum electron temperature enhancement, from near the reflection height, as a function of radar beam angle to the magnetic field for all the UHF antenna positions in Figure 1 between 1810 and 1946 UT which were pointed in the same direction as the HF beam. The electron temperature increase drops to half the field-aligned value when the HF beam is 5° further to the north, after which the decrease is much more gradual.

[22] Figure 6 shows the HF-induced electron temperature enhancements as a function of zenith angle for three separate directions of the HF beam from 1810 to 1946 UT, with the radar pointing in the same direction as the HF.

3.3. Remote Site Electron Temperatures

[23] One possible interpretation of the high electron temperatures measured along the field-aligned direction compared with other directions is that the electron temperature measurement is somehow invalid due to the effect of HF heating or that the temperature is anisotropic with a higher component along the magnetic field than perpendicular to it. Such anisotropies have been found for ion temperatures under strong natural ion-heating events [e.g., *Perraut et al.*, 1984; *Løvhaug and Flå*, 1986]. This would be surprising since the electron-neutral collision frequency is sufficiently high to isotropize the temperature. We can test this hypothesis by looking at the temperatures obtained from the remote site receivers at Kiruna, Sweden, and Sodankylä, Finland, whose antennas were pointing at the Tromsø beam at 250 km altitude. Figure 7 shows a scatterplot of the ratio of electron to ion temperatures measured at the height of 250 km by the remote sites Kiruna and Sodankylä for all antenna positions, versus the ratio measured at Tromsø. Clearly there is no significant difference in the ratio measured between the various sites. When Tromsø is measuring along the magnetic field, Kiruna and Sodankylä measure at 18° and 28° away from it, respectively. We also investigated the data from 16 February 1999, the event described by *Gustavsson et al.* [2001], and again found no difference between the temperature data from the three sites. Remote site electron temperatures during HF pumping measured by *Stocker et al.* [1992] were also consistent with the Tromsø data.

3.4. Electron Density Changes

[24] HF-induced electron density changes were more difficult to measure than the electron temperature changes for the following reasons. The density is much more variable both in time and space, and the artificial density changes are relatively small, usually less than 20%. This, together with the long heating cycle and the antenna movements, made the unheated background density profile measurement often displaced in time by 5–10 min from the heated profile so that the measurement of the artificial perturbation was often unreliable. Nevertheless, after examining the density perturbations from several profiles it is possible to conclude that above about 250 km the density decreases up to 20%, and below this height there may be a slight increase of a few percent. These results are slightly larger than but consistent with previous results from Tromsø [e.g., *Stocker et al.*, 1992; *Honary et al.*, 1993].

3.5. Radio-Induced Aurora

[25] Observations were made by the Digital All-Sky Imager (DASI) located near Skibotn, 50 km east and south of the HF facility [see *Kosch et al.*, 1998, 2000]. The 630 nm red $O(^1D)$ line was imaged with a 50° lens viewing in the vertical using an interference filter and a 10 s integration time. Optical conditions on 7 October 1999 were mostly cloudy at Skibotn, but the cloud thinned sufficiently between about 1846 and 1856 UT such that radio-induced aurora could be clearly observed when the HF beam was in the field-aligned position from 1848 to 1856 UT. There is also some weak radio-induced aurora at the start of the 6° position of the HF beam in the 1900 to 1908 UT cycle. The data quality is not good enough to give accurate emission intensities, but the position of the radio-induced aurora

Figure 3. (opposite) Two selected time intervals from 7 October 1999, showing electron density (Ne), ion and electron temperatures (Ti, Te), and ion velocity (Vi) from analyzed Tromsø long-pulse data for two field-aligned positions. (a) An interval starting about 3 minutes after HF pump on directed along the magnetic field, showing the largest elevated electron temperatures and ion outflows. (b) An interval starting about 3 minutes after HF pump off, showing the background values. The O^+ and M^+ (molecular ion) densities are from a model.

(a)

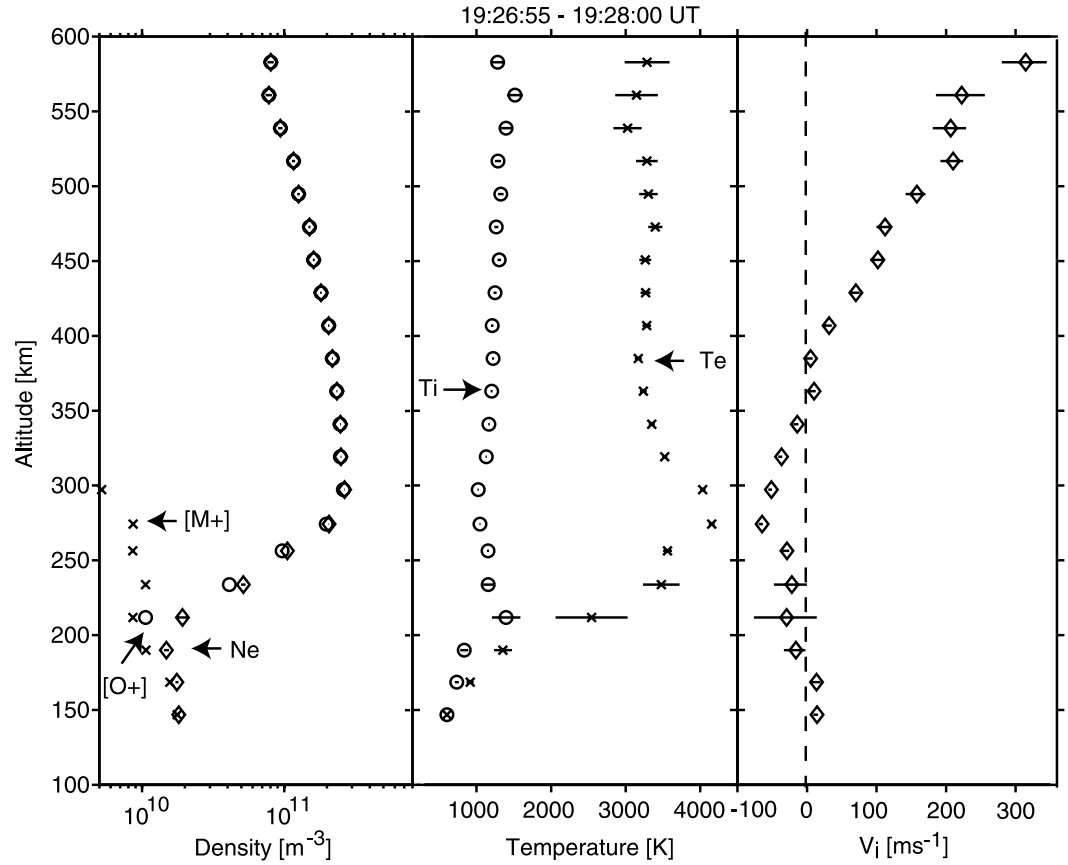
19:26:55 - 19:28:00 UT
Altitude [km]
600
550
500
450
400
350
300
250
200
150
100
[M+]
Ne
[O+]
Ti
Te
10^{10}
10^{11}
Density [m^{-3}]
1000 2000 3000 4000
Temperature [K]
-100 0 100 200 300
V_i [ms^{-1}]

(b)

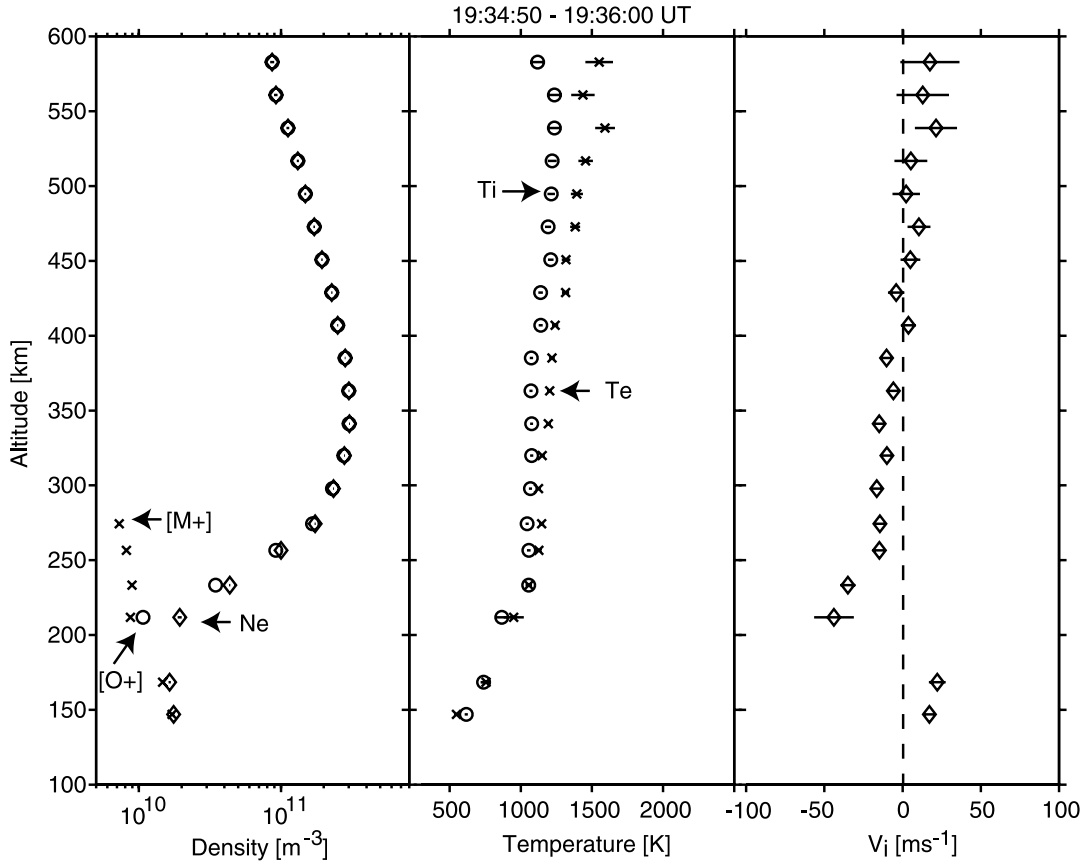
19:34:50 - 19:36:00 UT
Altitude [km]
600
550
500
450
400
350
300
250
200
150
100
[M+]
Ne
[O+]
Ti
Te
10^{10}
10^{11}
Density [m^{-3}]
500 1000 1500 2000
Temperature [K]
-100 -50 0 50 100
V_i [ms^{-1}]

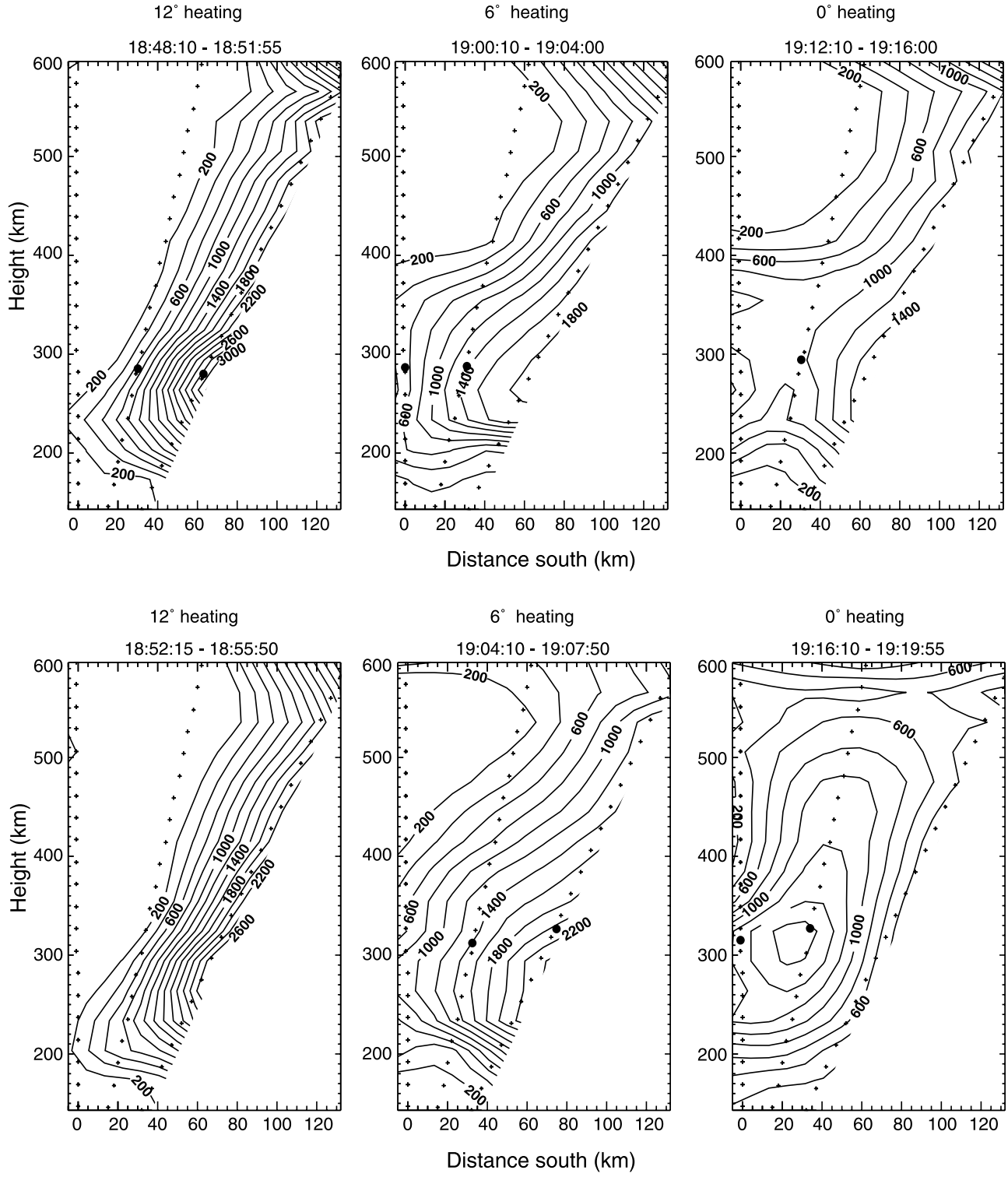

Figure 4. Contour plots of HF-induced electron temperature enhancements on 7 October 1999 for three positions of the HF-beam zenith angle, indicated at the top of each plot. Each plot is obtained from the analysis of long-pulse gates for three antenna positions. The centers of the gates are shown by the three lines of crosses. The background values which were subtracted from the data were obtained from the nearest time without heating but excluding the 6° position immediately after HF-off since that position still contains a heated plasma. The upper panels show the first four minutes while the lower panels show the second four minutes of each eight-minute HF pulse. The filled circles show the height of the HFIL.

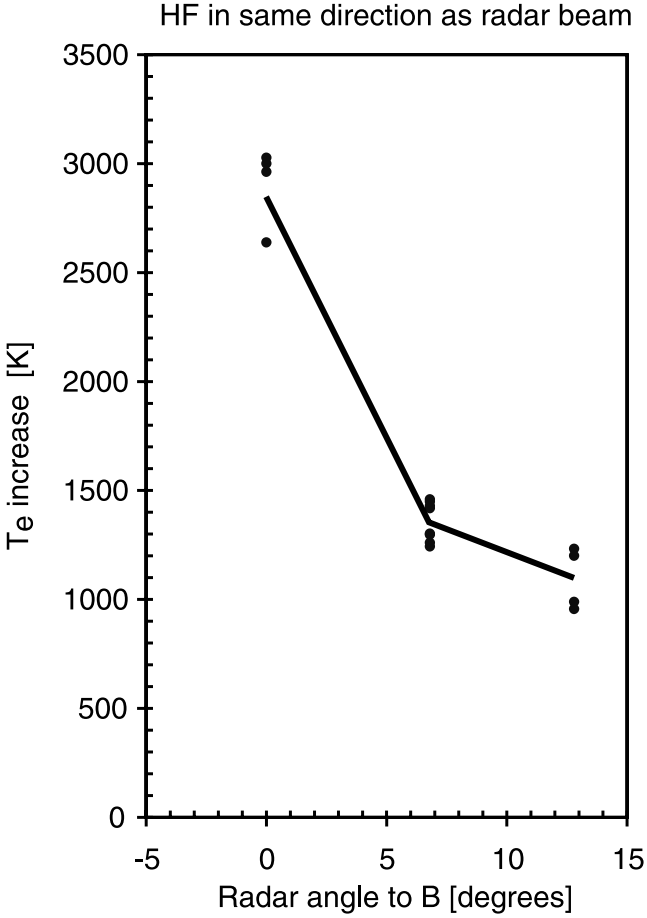

Figure 5. Electron temperature increase as a function of radar and HF angle to the Earth's magnetic field.

could be determined, as shown by the two images in Figure 8. The upper crosses mark the positions of the magnetic field line passing through the HF transmitter and intersecting the HF reflection altitude where the light is assumed to originate to a first approximation. The lower crosses show the vertical position from Ramfjordmoen. The ellipses show the −3 dB and −6 dB contours of the HF beam (for free space) for the two positions. That the free space approximation is reasonable, at least up to the upper hybrid resonance height, is shown later. Clearly, the radio-induced aurora patch does not move significantly between the two images even though the HF beam does. These observations support the conclusions given by *Kosch et al.* [2000, 2002b, 2003] that the auroral patch was seen displaced south of the main region illuminated by the HF beam when it was directed vertically. The fact that the electron temperatures also maximize in the same position as the observed light emission, irrespective of HF beam direction, suggest that the same mechanism, namely upper hybrid wave turbulence, is the cause of both phenomena and may also be taken as support for the hypothesis that the electron temperature enhancement is the main source of the red aurora. On the other hand, other observations [*Isham et al.*, 1999a] show that some aspects of Langmuir turbulence, which is not thought to be the main source of electron heating but which may excite energetic electrons, also show a preference for the field-aligned position. Many aspects of these observations are also not understood [*Isham et al.*, 1999a, 1999b].

3.6. HF Backscatter From Artificial Field-Aligned Irregularities

[26] Heating of the F region plasma causes artificial small-scale field-aligned irregularities (AFAI) or striations to be formed [*Fialer*, 1974; *Minkoff et al.*, 1974]. They have scale sizes between about one and several tens of meters. Diagnostics of the AFAI were made by two HF coherent radar systems.

3.6.1. HF Bistatic Backscatter

[27] A bistatic HF Doppler radio scatter experiment, the geometry of which is shown in Figure 1 of *Blagoveshchenskaya et al.* [1998], was carried out on the London-Tromsø-St. Petersburg path. The analysis of the received diagnostic waves, scattered from AFAI above Tromsø, was made by

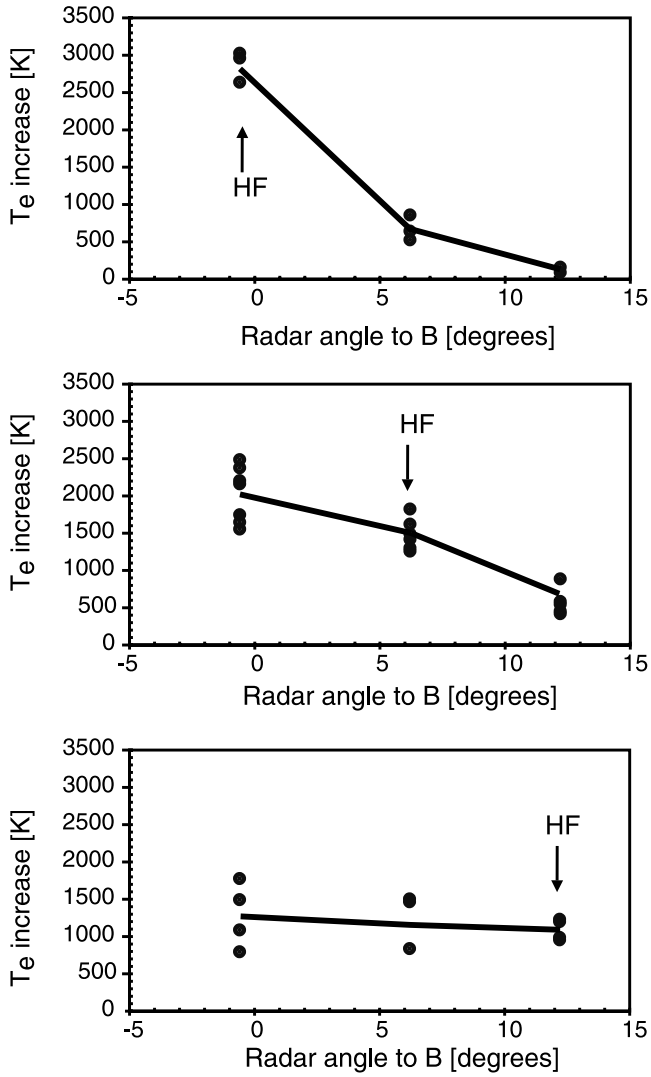

Figure 6. Electron temperature increase as a function of radar angle to the magnetic field, for three different HF-beam directions shown by the arrows. The HF beam is about 12° wide. The field-aligned radar position usually shows the largest enhancements.

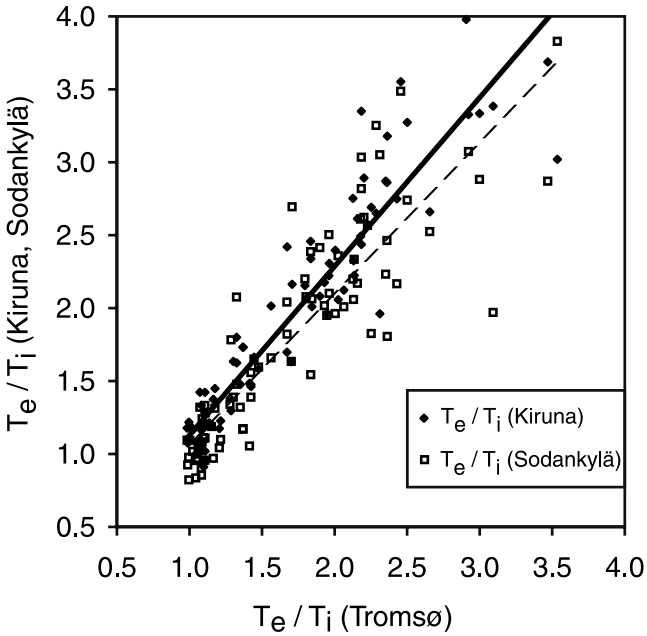

Figure 7. Scatter plot of the electron-to-ion-temperature ratios measured at the remote sites Kiruna (diamonds) and Sodankylä (squares) versus the ratio measured at Tromsø. The solid line is the best linear fit to the Kiruna data, the dashed line to the Sodankylä data. There is no significant bias from equal temperature ratios measured at all sites.

the Doppler spectral method in St. Petersburg at a distance of about 1200 km south of the Tromsø heating facility. Spectral processing of the diagnostic signals was made with a fast Fourier transform method. The frequency bandwidth used was 27 Hz with 256 spectral coefficients allowing a frequency resolution of about 0.1 Hz and temporal resolution of about 10 s. During the present experiment the bistatic HF Doppler radio scatter used the 12.095 MHz carrier signal from the BBC transmitter and therefore was sensitive to AFAI with spatial scales of 12.4 m perpendicular to the geomagnetic field.

[28] Figure 9a displays the dynamic Doppler spectra of HF diagnostic signals recorded in St. Petersburg in the course of three heating cycles from 1909 to 1945 UT. There were no backscatter signals observed from 1800 to 1848 UT. Observations were not made during the last 12 min of each hour because of interference from another sounder. From 1900 UT well-defined scattered signals were observed. Their spectral structure was quite similar to the heater-on period 1936–1944 UT, but the power was less. This HF-on period was not included in the HF Doppler plot because there was very strong interference between 1906 and 1907 UT. The behavior of power was similar to that observed by the CUTLASS Hankasalmi radar (see next section). The HF heater antenna beam was centered along vertical pointing (0°), field-aligned (12°) and Spitze angle (6°) during the first (1912–1920 UT), second (1924–1932 UT), and third (1936–1944 UT) heating cycle respectively. The field-aligned scattered signals appear after the heater is turned on and disappear after it is turned off. They are recorded as additional tracks on the negative part of Doppler sonogram shifted from that of the direct signal propagating from transmitter to the receiver along a great-cycle path and corresponding to the 0 Hz Doppler frequency. From Figure 9 it can be seen that signals scattered from AFAI are observed during all pumping cycles from 1909 to 1945 UT while the spectral structure of these signals depends on the zenith angle of the HF heater antenna beam. A broadening of the Doppler spectra as well as the Doppler frequency shifts of the scattered signals from direct HF signals peaked when the HF beam was centered along the field aligned pointing (12°).

[29] Figure 9b presents the temporal variations of the spectral power and the median values of the Doppler shift of the scattered HF signals calculated from the spectra shown in Figure 9a. One can recognize that the power of signals scattered from AFAI were also maximal under the heater

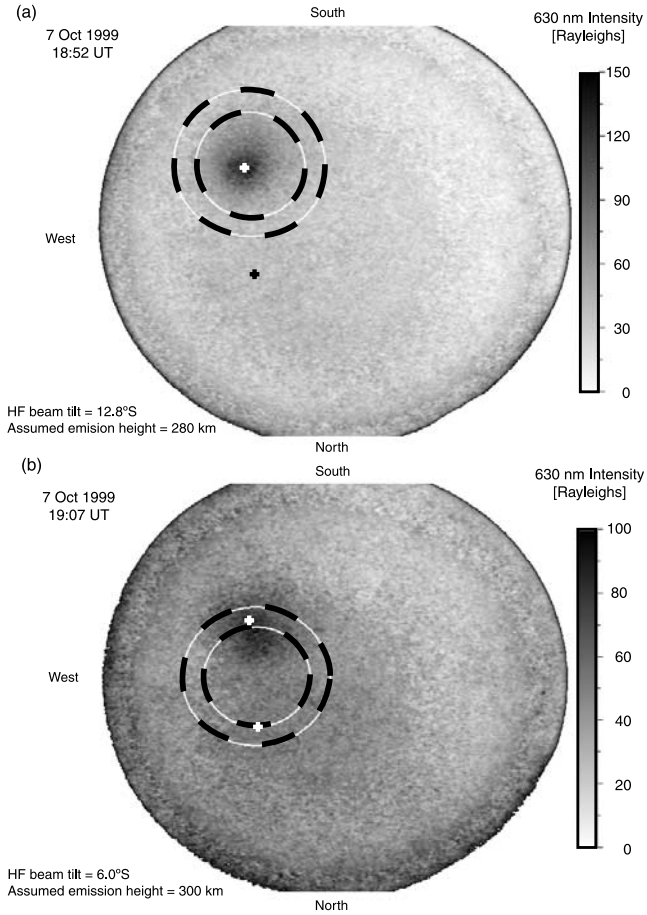

Figure 8. Images of 630 nm red light taken by a digital camera near Skibotn, for two intervals of HF-induced aurora. The dashed circles indicate the −3 dB (inner circle) and −6 dB (outer circle) contours of the HF beam mapped onto the assumed emission height assuming free space propagation. The upper white cross marks the intersection of the magnetic field line from the HF transmitter with the 280 km level, while the lower cross is the position overhead the HF facility. (a) 1848 to 1856 UT, with the HF beam tilted along the magnetic-field direction and an assumed emission height of 280 km. (b) 1900 to 1908 UT, with the HF beam tilted 6° south (Spitze) and an assumed emission height of 300 km.

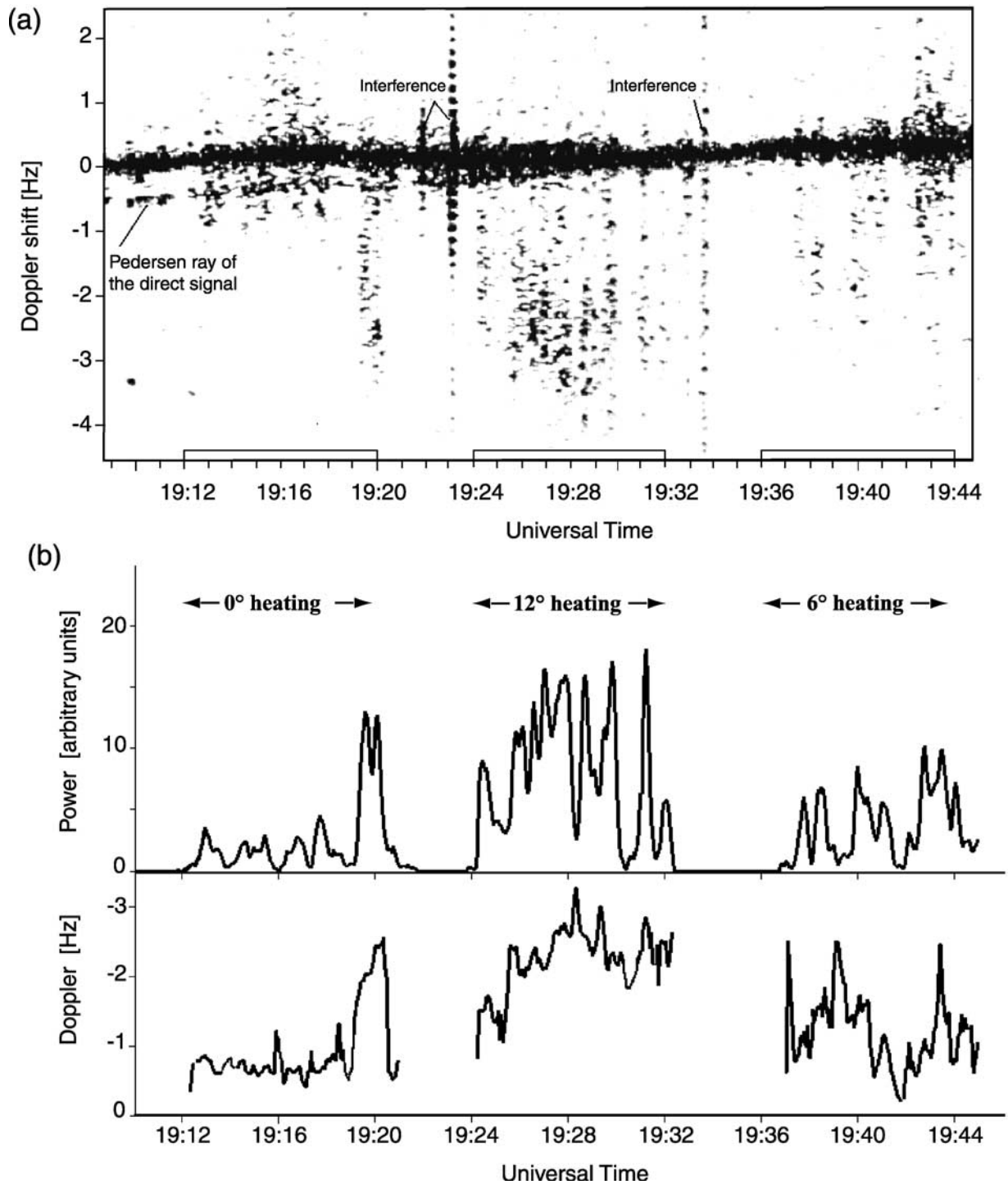

Figure 9. (a) Dynamic Doppler spectra of HF diagnostic signals on the London-Tromsø-St. Petersburg path at 12.095 MHz on 7 October 1999 from 1909 to 1945 UT. The direct signals propagating from the transmitter to the receiver along a great circle path correspond to zero Doppler shifts. The intervals when the Tromsø HF heater was turned on are marked on the time axis. During the first (1912–1920 UT), second (1924–1932 UT) and third (1936–1944 UT) heater-on periods the HF heater antenna beam was centered along vertical pointing (0° zenith angle), field-aligned (12°) and Spitze angle (6°), respectively. (b) Temporal variations of the spectral power (top panel) and median values of Doppler frequency shift (bottom panel) of the scattered HF signals calculated from the dynamic Doppler spectra shown in Figure 9a.

zenith angle of 12°. Therefore the spectral features of the scattered signals are strongly dependent on the elevation angles of the HF heater antenna beam. The spectral power, broadening of the Doppler spectra, and median values of Doppler Shift were maximal during the field aligned direction (12°) of the HF beam, whereas they were minimal during the vertical pointing (0°) of the HF beam.

3.6.2. HF Backscatter From CUTLASS

[30] The CUTLASS (Cooperative UK Twin Located Auroral Sounding System) radar is a pair of HF coherent backscatter radar systems located at Hankasalmi, Finland and Pykkvibær, Iceland and forms part of the SuperDARN array. Details of SuperDARN are given by *Greenwald et al.* [1995] and the CUTLASS systems at Hankasalmi and Pykkvibær by *Milan et al.* [1997]. CUTLASS is ideally situated for making observations of the power, spectral width, and Doppler shift of HF-induced AFAI over Tromsø [e.g., *Bond et al.*, 1997; *Eglitis et al.*, 1998]. Both Pykkvibær and Hankasalmi were in standard "common time" operations, with 45 km range gates, with the first range gate starting at a range of 180 km. Each beam was sampled for 7 s, with a full 16 beam scan being collected every 2 min. The radar frequencies were set for natural scatter, i.e., not optimized for the observation of heating effects over Tromsø, with both Hankasalmi and Pykkvibær set at 10.0 MHz after 1800 UT. Nevertheless the HF-induced backscatter was strong enough to be clearly distinguished on both radars. Figure 10 shows the backscattered power for the particular range and beam from each radar which covered the heated region.

[31] The Hankasalmi observations of artificial irregularities were colocated with ground scatter, but in spite of this enhanced power is visible up to 10 dB above that seen in the ground scatter for at least six heater on cycles. Pykkvibær observations are clearer, as no natural ionospheric or ground scatter was observed at the range of Tromsø, and the heater on periods raise the returned backscatter power up to 20 dB above the power observed during heater off periods. Examination of the angle of arrival of the Pykkvibær backscatter reveals it to have elevation angles of ~30°. This, and the range gate in which it is received, indicate that it is detected via a 2.5 hop HF propagation path as has been reported before [*Yeoman et al.*, 2001].

[32] There does not seem to be any clear dependence of the Iceland backscatter on the HF beam direction, apart from the strongest backscatter being seen at 1850 UT when the HF was pointed field-aligned. In the Finland data there seems to be a clearer pattern. The backscatter at 1930 UT (HF field-aligned) is stronger than at any other time, and correlates with the strong backscatter seen by the St. Petersburg diagnostic for that HF position. The backscatter at 1905 UT and 1940 UT (6° positions) is stronger than for the two positions where the HF is at 0° (1915 and 1950 UT). This also agrees with the St. Petersburg data in Figure 9 where the backscatter from 1937 to 1945 UT is stronger than 1912 to 1921 UT, the 0° position.

[33] Comparing the CUTLASS backscatter power with the data from EISCAT in Figure 1, we see that the onset of backscatter is correlated with both a general increase in the height of the HF-pump reflection height, as well as with a simultaneous increase in the electron temperature enhancement.

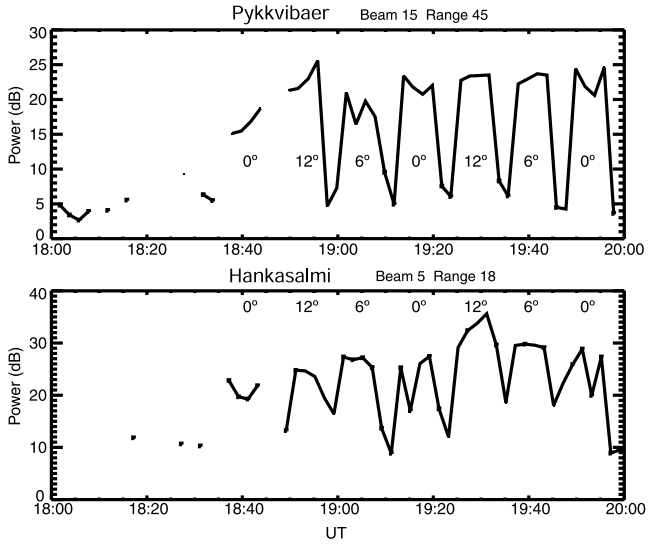

Figure 10. Backscattered power from the Pykkvibær (Iceland) and Hankasalmi (Finland) CUTLASS HF backscatter radars at 10 MHz on 7 October 1999. The beam and range correspond to the heated region above Tromsø. Both ground scatter and ionospheric scatter were observed at Hankasalmi. The numbers on the plot indicate the zenith angles of the HF-pump beam at Tromsø.

[34] In an independent study, *Dhillon* [2001] also found that the highest CUTLASS backscatter powers occurred to the south of the center of the heated patch, corresponding to the heater beam pointing in the field-aligned direction, indicating that field-aligned irregularities are generated most effectively in this direction.

4. Discussion

4.1. Field-Aligned Electron Temperatures and Ion Flows

[35] Modeling of the electron temperature enhancements caused by Ohmic heating was done by *Meltz and LeLevier* [1970] for the midlatitude case and by *Shoucri et al.* [1984] and *Hansen et al.* [1992] for the high-latitude ionosphere. Comparisons of models with experimental data were made by *Mantas et al.* [1981], *Newman et al.* [1988], and *Hansen et al.* [1992] for the midlatitude case and by *Robinson* [1989], *Stocker et al.* [1992], *Sergienko et al.* [2000], and *Gustavsson et al.* [2001] for the high-latitude cases, respectively. Modeling of the development and propagation of electron temperature and density perturbations along the magnetic field line has been done by *Vas'kov et al.* [1993] for the midlatitude ionosphere and by *Mingaleva and Mingalev* [1997] for the high-latitude situation. They predict ion outflows along the magnetic field caused by the electron heating, but to our knowledge they have not been reported before now. The physical mechanism is an increase of plasma pressure gradient caused by the electron heating which accelerates the plasma upwards. Detailed comparisons with the models are not attempted here but should be performed in the future.

4.2. Comparison With Other Observations at Tromsø

[36] One other case of large temperature enhancement associated with radio-induced aurora has been studied,

namely that of 16 February 1999 [*Leyser et al.*, 2000; *Sergienko et al.*, 2000; *Gustavsson et al.*, 2001]. In their case the radar measured constantly along the geomagnetic field while the HF beam was directed 6° south. The temporal development of the temperature changes are clearer in their case since the antenna beams remained stationary. Figure 3 of *Sergienko et al.* [2000] shows how the time constant of heating varies with height. Figure 1 of *Sergienko et al.* [2000] and Plate 8 of *Gustavsson et al.* [2001] show clearly how the temperature enhancement propagates upward along the field line. This would appear to be a solitary ion-acoustic compression wave that propagates along the magnetic flux tube from the heated region, as modeled for the Arecibo case by *Vas'kov et al.* [1993].

[37] We think that the large temperature increase observed in the nighttime experiments compared to the daytime results [e.g., *Stocker et al.*, 1992; *Honary et al.*, 1993] should be primarily attributed to the higher altitudes at night where the electron-neutral collision frequencies and therefore the heat losses are significantly lower. In all these results there remains the question as to how realistic are the measured temperatures. The incoherent scatter analysis assumes a uniform, Maxwellian plasma within the scattering volume. In some of the theories [e.g., *Gurevich et al.*, 1995] the striations contain plasma with very high electron temperatures with larger volumes between the striations with almost background temperatures. What does the incoherent scatter technique measure in this case? *Gurevich et al.* [1998] considered this question and suggested that when fitting only electron temperature, the mean square error of the fit should increase if strong heating in striations occurred. All we can say at present is that the residuals of the fits used to obtain the parameters in Figures 1 to 4 did not differ between the HF-heated and unheated times, but in our analysis all four standard parameters (electron density and temperature; ion temperature and velocity) were allowed to be fitted. Clearly, we need further studies to test the method of *Gurevich et al.* [1998] and perhaps new measurement techniques to resolve these issues.

4.3. HF-Ray Geometry

[38] The angle that the HF pump wave vector makes with the geomagnetic field is critical in determining the amount of HF energy available to excite AFAI. Only the component of the HF electric field that is perpendicular to the geomagnetic field ($E_\perp$) near the upper hybrid resonance level contributes to the excitation of the artificial field-aligned irregularities. For this reason it has been argued that anomalous heating effects and the associated AFAI are dominant at high latitudes where a vertically incident high power electromagnetic wave propagates at small angles to the magnetic field [*Robinson*, 1989]. To try to understand our results in detail we performed some ray tracing of the radio waves.

[39] The F region electron density profile was approximated by a parabolic function centered on 310 km with a width of 65 km. Ray tracing was done by calculating the Booker quartic [*Budden*, 1985] in 500 steps for each incident wave. The critical frequency was 4.9 MHz. Figure 11 shows a selection of ray paths with varying angles of incidence from the HF facility. The long-dash line shows the upper hybrid layer which is the height at which the HF pump frequency equals $(f_p^2 + f_c^2)^{1/2}$ where f_p is the plasma frequency and f_c is the gyro frequency. As can be seen from the figure, the dependence of $E_\perp$ on HF incident angle is very weak (a cosine dependence on angle of incidence) and cannot explain the strong dependence of temperature on HF angle.

[40] Figure 11 also shows that the ionosphere does not cause the HF wave to deviate very much from the free space path for rays incident with southward angles. The deviation from free space propagation is also minimal up to the UHR height for northward angles. This provides support for the mapping of the HF beam to near the reflection height in Figure 8 assuming free space propagation and a smooth, horizontally stratified ionosphere.

[41] A simple explanation for the southward bias may be the existence of a horizontal gradient in the electron density (as is natural near sunset) causing a tilt of our horizontally uniform ionosphere. For example, if the density gradient would be tilted 12° south instead of vertical, a wave transmitted field-aligned (and along the density gradient) would propagate up and down along the same path, thereby forming a standing wave pattern and have maximum electric field perpendicular to the magnetic field (to excite upper hybrid phenomena). Whatever the angle to the density gradient is, the standing wave pattern would be less smeared out the smaller the angle is between the transmitted HF wave vector and the density gradient.

[42] There were indeed horizontal gradients during this experiment, as can be seen by examining the electron density panels of Figures 1 and 2, but they were of different signs at different times. Before about 1850 UT the peak densities for the 13° south UHF antenna positions were lower than for overhead giving a northward tilt, whereas afterwards they were higher, resulting in a southward tilt. Calculations of the tilt at the upper-hybrid resonance height using the density profiles for the three positions gave absolute values typically between about 12° to 16° for both signs. Support for the ionospheric tilt explanation is given by the fact that the electron temperature enhancements along the field-aligned position seem to be much stronger than for the other positions after 1850 UT than before. The radio-induced aurora images in Figure 8 were also taken after 1850 UT. Nevertheless, the fact that the tilts were of different signs at different times argues against this explanation to explain the general trend. It is necessary to examine the relationship between ionospheric tilts and southward biases in HF pump-induced effects in much greater detail in the future.

[43] Another phenomenon which may be closely related is the observation by one of the authors (MTR, unpublished data) that natural ionospheric echoes from an HF sounder (NOAA dynasonde) located at the EISCAT facilities often show a southward bias close to the local magnetic field-line. To the authors' knowledge this effect is unexplained, and whether it is related to ionospheric tilts or multiple scattering off irregularities or both is under investigation.

4.4. Other Possible Explanations

[44] Another possible explanation for the directional dependence of the heating effects discussed here may be found by investigating the redistribution of electromagnetic energy density caused by multiple scattering of the HF

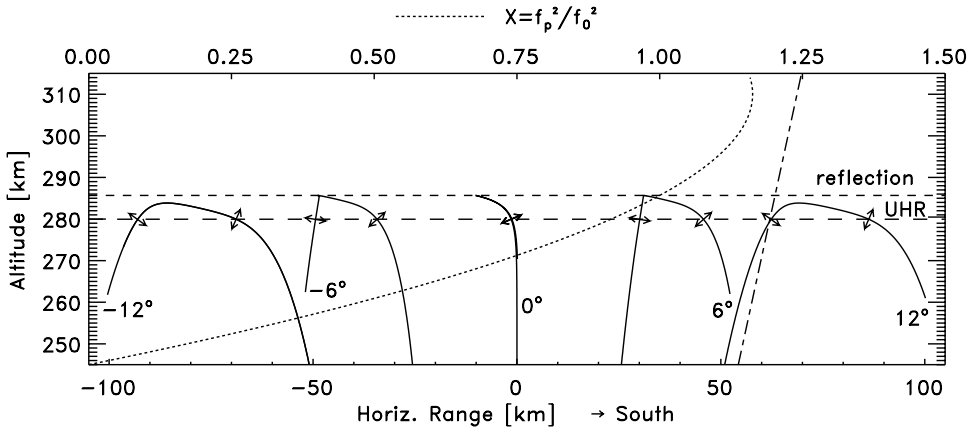

Figure 11. Schematic diagram of ray tracing HF waves of varying angles of incidence into a horizontally uniform ionosphere. The ionospheric electron density profile is shown by the curved dotted line and relates to the upper X-axis, which is normalised to the pump frequency of 4.544 MHz. The reflection height and upper-hybrid resonance (UHR) heights are shown labeled and the wave electric field direction of the upward and downward going waves at the UHR height are shown by arrows. The magnetic field direction is shown as a dash-dotted line. Efficient HF-induced heating is expected where the wave electric field is perpendicular to the magnetic field such that coupling to upper-hybrid waves is most efficient.

waves by intermediate scale (0.1–1 km) irregularities. Such scattering has been used to explain anomalous attenuation of HF waves and its directional dependence [*Zabotin et al.*, 1998, 2002; *Zabotin and Kovalenko*, 1999].

[45] The minutes-long heating cycles used in this experiment will also cause large scale changes in the electron density distribution which could cause nonlinear refraction effects as discussed by *Hansen et al.* [1992]. Self-focusing effects [e.g., *Bernhardt and Duncan*, 1982] may also be important. Whether these can explain a southward bias of the observed effects is open to further research, but we note that *Hansen et al.* [1992] found that nonlinear refraction resulted in a northward shift of the most heated region for the Arecibo case, which is opposite to what we find. Nevertheless, the effects of HF-induced electron density changes on the refractive index surfaces for the high-latitude case should be examined.

[46] A promising explanation seems to be self-focusing of the HF wave caused by the density depletions within the striations, as examined by *Gurevich et al.* [2001] to explain the southward bias in HF-induced airglow. In this model striations are formed which trap upper-hybrid waves in the direction perpendicular to the magnetic field leading to electron energization and an overall density depletion within the striations.

[47] In the model of *Istomin and Leyser* [2001] there is a diffraction of the HF wave on the small-scale striations. Whether development of this theory can explain the preference for rays propagating along the magnetic field to be more unstable to upper-hybrid turbulence remains to be seen.

[48] If these models with enhanced temperatures inside striations apply, then one has to ask how the electron temperature and density measured by the incoherent scatter technique, which assumes a uniform plasma in thermal equilibrium within the scattering volume (several kilometers in both diameter and in height), relate to the actual values which vary by a large factor between the volume within the striations and that outside. In a simplistic approach one might think that our incoherent scatter results are an average for the volume measured which would imply that the actual electron temperatures within the striations were 10000 K or more.

5. Conclusions

[49] Electron temperature enhancements of up to 3000 K induced by powerful HF pumping at night in the quiet high-latitude ionosphere have been measured. They spread along the field line up to the highest measured altitude of nearly 600 km. Associated with them are field-aligned ion outflows of up to several hundred meters per second. The ion temperature changes by only a few hundred Kelvin and small electron density depletions of up to 20% occur near the interaction height. The electron temperature enhancements induced by powerful HF pumping show a strong dependence on the angle of the HF pumping waves to the Earth's magnetic field. The strongest effects are for rays propagating near parallel to the magnetic field. This is consistent with observations of HF-induced aurora seen in the 630 nm (O^1D) line which is also preferentially excited by HF rays in the same direction. There are indications from independent HF backscatter radars that meter-scale field-aligned irregularities also produce stronger backscatter when pumping in the magnetic field-aligned direction. Electron heating, probably 630 nm radio-induced aurora, anomalous absorption, and striation formation are all thought to be produced through upper-hybrid wave turbulence which is excited by pump electric fields perpendicular to the geomagnetic field. Such a strong dependence of upper-hybrid related phenomena on HF aspect angle is unexpected and not understood.

[50] Possible explanations for this angular dependence are ionospheric tilts, multiple scattering off small-scale irregularities, or self-focusing or diffraction of the HF waves on field-aligned striations causing the energy to be distrib-

uted asymmetrically. There is evidence that ionospheric tilts existed during these observations but how important they are is unclear.

[51] To better measure the range of optimum coupling angles it is desirable to repeat such scanning experiments using a narrower HF beam, for example using array 1 (sometimes termed "superheater") of the Tromsø facility, and scanning the UHF antenna in smaller steps and beyond the field-aligned position. Further measurements of ionospheric tilts and studies of their effect on ionospheric heating are necessary. It would be interesting to see whether other spectral lines of artificially excited optical emissions and the stimulated electromagnetic emission (SEE) phenomenon also exhibit a directional dependence like many of the effects discussed here. This, together with experiments which determine the gyrofrequency dependence of the various auroral emissions, should help determine which mechanism is responsible for the various phenomena.

[52] **Acknowledgments.** We thank Philippe Gamet and Stephan Buchert for making available plotting routines and Harry Kohl for the raytracing routine. The EISCAT Scientific Association is supported by Suomen Akatemia of Finland, Centre National de la Recherche Scientifique of France, Max-Planck-Gesellschaft of Germany, the National Institute of Polar Research of Japan, Norges Forskningsråd of Norway, the Swedish Research Council, and the Particle Physics and Astronomy Research Council of the United Kingdom. The work of N. B and V. K. was partially sponsored by NATO Collaborative Linkage grant CLG 978226 and the Russian Foundation of Fundamental Research, grant 00-05-64819. We thank B. Isham for useful comments.

[53] Arthur Richmond thanks A. V. Gurevich and Alice L. Newman for their assistance in evaluating this paper.

References

Bernhardt, P. A., and L. M. Duncan, The feedback-diffraction theory of ionospheric heating, *J. Atmos. Terr. Phys.*, *44*, 1061–1074, 1982.

Bernhardt, P. A., M. Wong, J. D. Huba, B. G. Fejer, L. S. Wagner, J. A. Goldstein, C. A. Selcher, V. L. Frolov, and E. N. Sergeev, Optical remote sensing of the thermosphere with HF pumped artificial airglow, *J. Geophys. Res.*, *105*, 10,657–10,671, 2000.

Blagoveshchenskaya, N. F., V. A. Kornienko, A. V. Petlenko, A. Brekke, and M. T. Rietveld, Geophysical phenomena during an ionospheric modification experiment at Tromsø, *Ann. Geophys.*, *16*, 1212–1225, 1998.

Bond, G. E., T. R. Robinson, P. Eglitis, D. M. Wright, A. J. Stocker, M. T. Rietveld, and T. B. Jones, Spatial observations by the CUTLASS coherent scatter radar of ionospheric modification by high power radio waves, *Ann. Geophys.*, *15*, 1412–1421, 1997.

Brändström, B. U. E., T. B. Leyser, Å. Steen, M. T. Rietveld, B. Gustavsson, T. Aso, and M. Ejiri, Unambiguous evidence of HF pump-enhanced airglow at auroral latitudes, *Geophys. Res. Lett.*, *26*, 3561–3564, 1999.

Budden, K. G., *The Propagation of Radio Waves*, 669 pp., Cambridge Univ. Press, New York, 1985.

Dhillon, R. S., Radar studies of natural and artificial waves and instabilities in the auroral ionosphere, Ph.D. thesis, Univ. of Leicester, Leicester, U.K., 2001.

Djuth, F. T., B. Thidé, H. M. Ierkic, and M. P. Sulzer, Large F region electron-temperature enhancements generated by high-power HF radio waves, *Geophys. Res. Lett.*, *14*, 953–956, 1987.

Duncan, L. M., J. P. Sheerin, and R. A. Behnke, Observations of ionospheric cavities generated by high-power radio waves, *Phys. Rev. Lett.*, *61*, 239–242, 1988.

Eglitis, P., T. R. Robinson, M. T. Rietveld, D. M. Wright, and G. E. Bond, The phase speed of artificial field-aligned irregularities observed by CUTLASS during HF modification of the auroral ionosphere, *J. Geophys. Res.*, *103*, 2253–2259, 1998.

Fialer, P. A., Field-aligned scattering from a heated region of the ionosphere- Observations at HF and VHF, *Radio Sci.*, *9*, 923–940, 1974.

Franz, T. L., M. C. Kelly, and A. V. Gurevich, Radar backscattering from artificial field-aligned irregularities, *Radio Sci.*, *34*, 465–475, 1999.

Gordon, W. E., and H. C. Carlson Jr., Arecibo heating experiments, *Radio Sci*, *9*, 1041–1047, 1974.

Gordon, W. E., H. C. Carlson, and R. L. Showen, Ionospheric heating at Arecibo: First tests, *J. Geophys. Res.*, *76*, 7808–7813, 1971.

Grach, S. M., and V. Y. Trakhtengerts, Parametric excitation of ionospheric irregularities extended along the magnetic field line, *Radiophys. Quantum Electron.*, *18*, 951–957, 1976.

Greenwald, R. A., et al., DARN/SUPERDARN: A global view of the dynamics of high-latitude convection, *Space Sci. Rev.*, *71*, 761–796, 1995.

Gurevich, A. V., and G. M. Milikh, Artificial airglow due to modifications of the ionosphere by powerful radio waves, *J. Geophys. Res.*, *102*, 389–394, 1997.

Gurevich, A. V., A. V. Lukyanov, and K. P. Zybin, Stationary state of isolated striations developed during ionospheric modification, *Phys. Lett. A*, *206*, 247–259, 1995.

Gurevich, A. V., A. V. Lukyanov, and K. P. Zybin, Anomalous absorption of powerful radio waves on the striations developed during ionospheric modification, *Phys. Lett. A*, *211*, 363–372, 1996.

Gurevich, A. V., T. Hagfors, H. Carlson, A. V. Lukyanov, and K. P. Zybin, Electron temperature measurements by incoherent scattering in the presence of strong small scale temperature irregularities, *Phys. Lett. A*, *246*, 335–340, 1998.

Gurevich, A. V., H. Carlson, M. Kelley, T. Hagfors, A. Karashtin, and K. P. Zybin, Nonlinear structuring of the ionosphere modified by powerful radio waves at low latitudes, *Phys. Lett. A*, *251*, 311–321, 1999.

Gurevich, A. V., H. Carlson, and K. P. Zybin, Nonlinear structuring and southward shift of a strongly heated region in ionospheric modification, *Phys. Lett. A*, *288*, 231–239, 2001.

Gustavsson, B., et al., First tomographic estimate of volume distribution of HF-pump enhanced airglow emission, *J. Geophys. Res.*, *106*, 29,105–29,124, 2001.

Hansen, J. D., G. J. Morales, and J. E. Maggs, Large-scale HF-induced ionospheric modifications: theory and modeling, *J. Geophys. Res.*, *97*, 17,019–17,032, 1992.

Honary, F., A. J. Stocker, T. R. Robinson, T. B. Jones, N. M. Wade, P. Stubbe, and H. Kopka, EISCAT observations of electron temperature oscillations due to the action of high power HF radio waves, *J. Atmos. Terr. Phys.*, *55*(10), 1433–1448, 1993.

Honary, F., A. J. Stocker, T. R. Robinson, T. B. Jones, and P. Stubbe, Ionospheric plasma response to HF radio waves operating at frequencies close to the third harmonic of the electron gyrofrequency, *J. Geophys. Res.*, *100*, 21,489–21,502, 1995.

Isham, B., M. T. Rietveld, T. Hagfors, C. La Hoz, E. Mishin, W. Kofman, T. B. Leyser, and A. P. van Eyken, Aspect angle dependence of HF enhanced incoherent backscatter, *Adv. Space Res.*, *24*, 1003–1006, 1999a.

Isham, B., T. Hagfors, E. Mishin, M. Rietveld, C. LaHoz, W. Kofman, and T. Leyser, A search for the location of the HF excitation of enhanced ion acoustic and Langmuir waves with EISCAT and the Tromsø heater, *Radiophys. Quantum Electron.*, *42*, 607–618, 1999b.

Istomin, Y. N., and T. B. Leyser, Small-scale magnetic field-aligned density irregularities excited by a powerful electromagnetic wave, *Phys. Plasmas*, *4*, 817–828, 1997.

Istomin, Y. N., and T. B. Leyser, Diffraction of electromagnetic waves by small scale geomagnetic field-aligned density striations, *Phys. Plasmas*, *8*, 4577–4584, 2001.

Jones, T. B., T. R. Robinson, P. Stubbe, and H. Kopka, EISCAT observations of the heated ionosphere, *J. Atmos. Terr. Phys.*, *48*, 1027–1035, 1986.

Kelley, M. C., T. L. Arce, J. Salowey, M. Sulzer, W. T. Armstrong, M. Carter, and L. Duncan, Density depletions at the 10-m scale induced by the Arecibo heater, *J. Geophys. Res.*, *100*, 17,367–17,376, 1995.

Kosch, M. J., T. Hagfors, and E. Nielsen, A new digital all-sky imager experiment for optical auroral studies in conjunction with the Scandinavian twin auroral radar experiment, *Rev. Sci. Inst.*, *69*, 578–584, 1998.

Kosch, M. J., M. T. Rietveld, T. Hagfors, and T. B. Leyser, High-latitude HF-induced airglow displaced equatorwards of the pump beam, *Geophys. Res. Lett,.*, *27*, 2817–2820, 2000.

Kosch, M. J., M. T. Rietveld, A. J. Kavanagh, C. Davis, T. Yeoman, F. Honary, and T. Hagfors, High-latitude pump-induced optical emissions for frequencies close to the third electron gyro-harmonic, *Geophys. Res. Lett.*, *29*(23), 2112, doi:10.1029/2002GL015744, 2002a.

Kosch, M. J., M. T. Rietveld, T. Yeoman, K. Cierpka, and T. Hagfors, The high-latitude artificial aurora of 21 February 1999: An analysis, *Adv. Polar Upper Atmos. Res.*, *16*, 1–12, 2002b.

Kosch, M. J., M. T. Rietveld, F. Honary, and T. Hagfors, High-latitude artificial aurora from EISCAT: A unique phenomenon?, *28th Annual Optical Meeting Conference Proceedings*, Univ. of Oulu, Finland, in press, 2003.

Leyser, T. B., B. U. E. Brändström, B. Gustavsson, Å. Steen, F. Honary, M. T. Rietveld, T. Aso, and M. Ejiri, Simultaneous measurements of high-frequency pump-enhanced airglow and ionospheric temperatures at auroral latitudes, *Adv. Polar Upper Atmos. Res.*, *14*, 1–11, 2000.

Løvhaug, U. P., and T. Flå, Ion temperature anisotropy in the auroral F region as measured with EISCAT, *J. Atmos. Terr. Phys.*, *48*, 959–971, 1986.

Mantas, G. P., Large 6300-Å airglow intensity enhancements observed in ionosphere heating experiments are excited by thermal electrons, *J. Geophys. Res.*, *99*, 8993–9002, 1994.

Mantas, G. P., and H. C. Carlson, Reinterpretation of the 6300-Å airglow enhancements observed in ionosphere heating experiments based on analysis of Platteville, Colorado, data, *J. Geophys. Res.*, *101*, 195–209, 1996.

Mantas, G. P., H. C. Carlson Jr., and C. H. LaHoz, Thermal response of the F region ionosphere in artificial modification experiments by HF radio waves, *J. Geophys. Res.*, *86*, 561–574, 1981.

Meltz, G., and R. E. LeLevier, Heating the F region by deviative absorption of radio waves, *J. Geophys. Res.*, *75*, 6406–6416, 1970.

Milan, S. E., T. K. Yeoman, M. Lester, E. C. Thomas, and T. B. Jones, Initial backscatter occurrence statistics from the CUTLASS HF radars, *Ann. Geophys.*, *15*, 703–718, 1997.

Minkoff, J., P. Kugelman, and I. Weissman, Radio frequency scattering from a heated ionospheric volume, 1, VHF/UHF field-aligned and plasma-line backscatter measurements, *Radio Sci.*, *9*, 941–955, 1974.

Mingaleva, G. I., and V. S. Mingalev, Response of the convecting high-latitude F layer to a powerful HF wave, *Ann. Geophys.*, *15*, 1291–1300, 1997.

Mishin, E., H. Carlson, and T. Hagfors, On the electron distribution function in the F region and airglow enhancements during HF modification experiments, *Geophys. Res. Lett.*, *27*, 2857–2860, 2000.

Mishin, E., T. Hagfors, and B. Isham, A generation mechanism for topside enhanced incoherent backscatter during high frequency modification experiments in Tromsø, *Geophys. Res. Lett.*, *28*, 479–482, 2001.

Newman, A. L., H. C. Carlson Jr., G. P. Mantas, and F. T. Djuth, Thermal response of the F region ionosphere for conditions of large HF-induced electron-temperature enhancements, *Geophys. Res. Lett.*, *15*, 311–314, 1988.

Pedersen, T. R., and H. C. Carlson, First observations of HF heater-produced airglow at the High Frequency Active Auroral Research facility: Thermal excitation and spatial structuring, *Radio Sci.*, *36*, 1013–1026, 2001.

Perraut, S., A. Brekke, M. Baron, and D. Hubert, EISCAT measurements of ion temperatures which indicate non-isotropic ion velocity distributions, *J. Atmos. Terr. Phys.*, *46*, 531–543, 1984.

Ponomarenko, P. V., T. B. Leyser, and B. Thidé, New electron gyroharmonic effects in HF scatter from pump-excited magnetic field-aligned ionospheric irregularities, *J. Geophys. Res.*, *104*, 10,081–10,087, 1999.

Rietveld, M. T., H. Kohl, H. Kopka, and P. Stubbe, Introduction to ionospheric heating experiments at Tromsø, 1, Experimental overview, *J. Atmos. Terr. Phys.*, *55*, 577–599, 1993.

Rietveld, M. T., B. Isham, H. Kohl, C. La Hoz, and T. Hagfors, Measurements of HF-enhanced plasma and ion lines at EISCAT with high altitude resolution, *J. Geophys. Res.*, *105*, 7429–7439, 2000.

Robinson, T. R., The heating of the high latitude ionosphere by high power radio waves, *Phys. Rep.*, *179*, 79–209, 1989.

Robinson, T. R., F. Honary, A. J. Stocker, T. B. Jones, and P. Stubbe, First EISCAT observations of the modification of F region electron temperatures during RF heating at harmonics of the electron gyrofrequency, *J. Atmos. Terr. Phys.*, *58*, 385–395, 1996.

Sergienko, T., B. Gustavsson, Å. Steen, U. Brändström, M. T. Rietveld, T. B. Leyser, and F. Honary, Analysis of excitation of the 630.0 nm airglow during a heating experiment in Tromsø on February 16, 1999, *Phys. Chem. Earth*, *25*, 531–535, 2000.

Shoucri, M. M., G. J. Morales, and J. E. Maggs, Ohmic heating of the polar F region by HF pulses, *J. Geophys. Res.*, *89*, 2907–2917, 1984.

Stocker, A. J., F. Honary, T. R. Robinson, T. B. Jones, P. Stubbe, and H. Kopka, EISCAT observations of large scale electron temperature and electron density perturbations caused by high power HF radio waves, *J. Atmos. Terr. Phys.*, *54*, 1555–1572, 1992.

Vas'kov, V. V., and A. V. Gurevich, Nonlinear resonant instability of a plasma in the field of an ordinary electromagnetic wave, *Sov. Phys. JETP (Engl. Transl.)*, *42*, 91–97, 1976.

Vas'kov, V. V., Y. S. Dimant, and N. A. Ryabova, Magnetospheric plasma thermal perturbations induced by resonant heating of the ionospheric F region by high-power radio wave, *Adv. Space Res.*, *13*, 25–33, 1993.

Yeoman, T. K., D. M. Wright, A. J. Stocker, and T. B. Jones, An evaluation of range accuracy in the SuperDARN over-the-horizon HF radar systems, *Radio Sci.*, *36*, 801–813, 2001.

Zabotin, N. A., A. G. Bronin, and G. A. Zhbankov, Radiative transfer in a layer of magnetized plasma with random irregularities, *Waves Random Media*, *8*, 421–436, 1998.

Zabotin, N. A., and E. S. Kovalenko, Simple numerical model of radio wave multiple scattering effects in the ionospheric plasma layer, *Waves Random Media*, *9*, 393–399, 1999.

Zabotin, N. A., A. G. Bronin, V. L. Frolov, G. P. Komrakov, N. A. Mityakov, E. N. Sergeev, and G. A. Zhbankov, Anomalous attenuation of extraordinary waves in the ionosphere heating experiments, *Radio Sci.*, *37*(6), 1102, doi:10.1029/2000RS002609, 2002.

N. F. Blagoveshchenskaya and V. A. Kornienko, Arctic and Antarctic Research Institute, 38 Bering Str., 199397 St. Petersburg, Russia. (nataly@aari.nw.ru; vikkorn@aari.nw.ru)

M. J. Kosch, Communication Systems, Lancaster University, LA1 4YR Lancaster, UK. (m.kosch@lancaster.ac.uk)

T. B. Leyser, Swedish Institute of Space Physics, Bos 537, SE-571 21 Uppsala, Sweden. (tbl@irfu.se)

M. T. Rietveld, Max-Planck Institut für Aeronomie, 37191 Katlenburg-Lindau, Germany. (rietveld@linmpi.mpg.de)

T. K. Yeoman, Physics and Astronomy, Leicester University, Leicester LE1 7RH, UK. (tim.yeoman@ion.le.ac.uk)